

THE STUDY OF ATMOSPHERE OF HOT JUPITERS AND THEIR HOST STARS

M. C. Maimone¹, A. Chiavassa¹ and J. Leconte²

Abstract. What makes the study of exoplanetary atmospheres so hard is the extraction of its tiny signal from observations, usually dominated by telluric absorption, stellar spectrum and instrumental noise. The High Resolution Spectroscopy has emerged as one of the leading techniques for detecting atomic and molecular species (Birkby 2018), but although it is particularly robust against contaminant absorption in the Earth's atmosphere, the non-stationary stellar spectrum — in the form of either Doppler shift or distortion of the line profile during planetary transits — creates a non-negligible source of noise that can alter or even prevent the detection. Recently, significant improvements have been achieved by using 3D, radiative hydrodynamical (RHD) simulations for the star and Global Circulation Models (GCM) for the planet (e.g., Chiavassa & Brogi 2019, Flowers et al. 2019). However, these numerical simulations have been computed independently so far, while acquired spectra are the result of the natural coupling at each phase along the planet orbit. With our work, we aim at generating emission spectra of G,F, and K-type stars and Hot Jupiters and coupling them at any phase of the orbit. This approach is expected to be particularly advantageous for those molecules that are present in both the atmospheres (e.g., CO) and form in the same region of the spectrum, resulting in mixed and overlapped spectral lines. We also present the analysis of transmission spectra of the Hot Saturn WASP-20b, observed in the K-band of the recently upgraded spectrograph VLT/CRIRES+ at a resolution $R \sim 92,000$ during the first night of the Science Verification of the instrument and that led to a tentative detection of H₂O.

Keywords: Planets and satellites: atmospheres, Stars: atmospheres, Techniques: spectroscopic

1 Introduction

High-resolution spectroscopy (HRS) at resolving powers $R > 50\,000$ has proved to be one of the leading technique for remote atmospheric characterisation of exoplanet atmospheres. HRS allows to partially resolve the molecular dense forest of lines and to robustly identify them through line-matching techniques such as cross-correlation (Snellen et al. 2010). This technique occurred to be particularly suitable in the Near-Infrared due to a favourable planet-to-star flux contrast ratio and to the presence of strong absorption bands of the main carriers of carbon (CO) and oxygen (H₂O) (Madhusudhan 2012).

Although several molecules (CO, H₂O, CH₄, HCN, TiO) have been detected in the atmosphere of a dozen exoplanets (Birkby 2018 for a review), characterizing an exoplanet remains a challenge. Stars are non-uniform and can be potential source of spurious signals, which can alter or even prevent the interpretation of exoplanet spectra (Chiavassa et al. 2017; Cegla et al. 2019; Chiavassa & Brogi 2019; Dravins et al. 2021). In particular, the granulation pattern associated with the heat transport by convection (Nordlund et al. 2009) has a temporal and spatial variability which manifests as Doppler shifts and distortions of the line profile (Fig. 1, top panels) during the planetary transit. Similarly, atmospheric circulation and planetary winds affect the planetary spectrum (Fig. 1, bottom panels), causing an overlap of effects of similar time-scales (Flowers et al. 2019).

In this context, the use of 3D, radiative hydrodynamical (RHD) simulations for stars and Global Circulation Models (GCM) for planets play a major role (e.g., Chiavassa & Brogi 2019 and yet, so far they have been computed independently, while acquired spectra are the result of the natural coupling at each phase along the planet orbit.

¹ Université Côte d'Azur, Observatoire de la Côte d'Azur, CNRS, Lagrange, CS 34229, Nice, France

² Laboratoire d'astrophysique de Bordeaux, Univ. Bordeaux, CNRS, B18N, allée Geoffroy Saint-Hilaire, 33615 Pessac, France

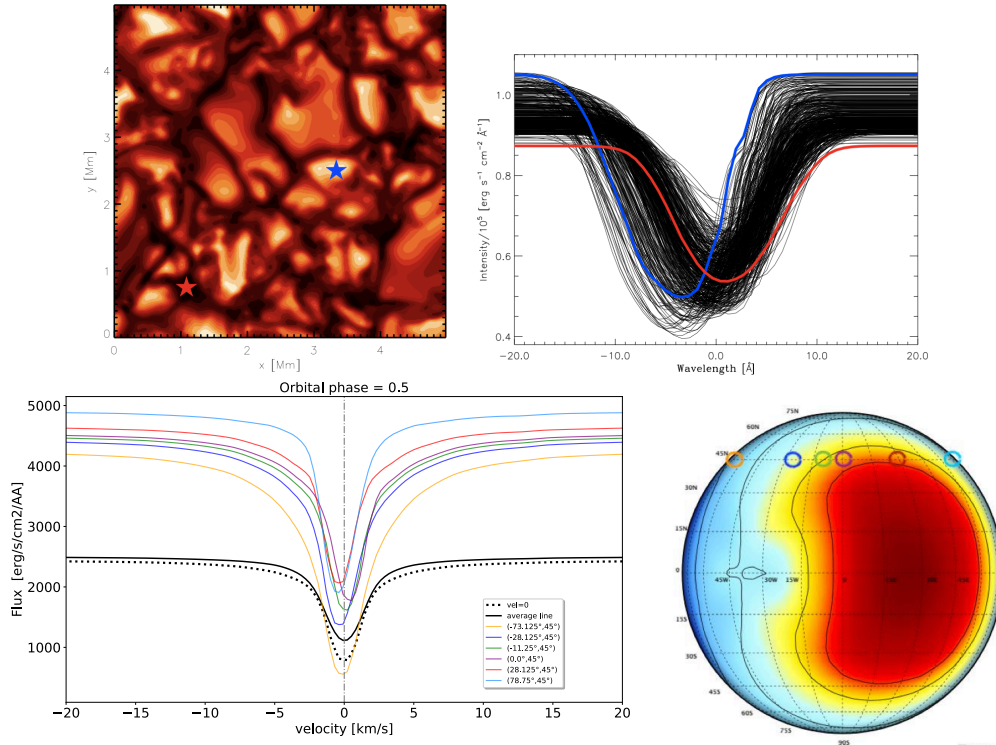


Fig. 1. *Top panels:* Intensity maps of a K-dwarf simulation at disk center (left) and the corresponding spatially resolved profiles of one CO line across the granulation pattern (Chiavassa & Brogi 2019) (right). The solid red (intergranular lane) and blue (granule) lines displays two particular positions (colored star symbols) extracted from the intensity map. *Bottom panels:* One particular Hot Jupiter CO line computed for different atmospheric regions (left), which are marked by circles with same colors in the corresponding intensity map (right).

2 The two side of the project

2.1 Emission spectroscopy: synthetic observables and the study of detectability of the planet signal

We are developing a new approach which aims at generating high resolution emission spectra of Hot Jupiters (1400K-2100K) and their host star (G,F,K-type) combined along the orbit to reproduce realistic synthetic observations. The innovation and uniqueness of this approach is the use of 3D hydrodynamical simulations for the atmosphere of both the star (STAGGER-CODE, Nordlund et al. 2009; Magic et al. 2013) and the planet (MITgcm Showman et al. 2013; Parmentier et al. 2021). Two summary grids are given in Fig. 2, left and central panels, respectively. The coupling is done by using an updated version of the post-processing radiative transfer code OPTIM3D (Chiavassa et al. 2009). The code takes into account, simultaneously, the stellar and planetary dynamics, which influence the shape, shift, and asymmetries of spectral lines, and not rarely of the same specie. We will perform a study of detectability of the planet signal by exploring the coupling grid (right panel of Fig. 2) to understand if any other star-planet couple can reproduce the same signal of the input one.

With the new generation of telescopes (e.g., CAHA/CARMENES, VLT/CRILES+, CHFT/SPIROU, ELT, etc,...) and the increasing number of planets expected to be observed, our tool will be extremely useful to interpret HRS data to extract information either for the characterization of the stellar parameters and metallicity and for the planet dynamics and composition.

2.2 Transmission spectroscopy: tentative detection of H₂O in the atmosphere of WASP-20b

We present the analysis of transmission spectra of the inflated, Saturn-mass planet WASP-20b (0.31 M_J; 1.46 R_J) orbiting a F9-type star in less than 5 days and with an equilibrium temperature of ~1400K (Maimone et al. 2022, submitted). Our observations occurred on Sept, 16 2021, during the very first night of the Science Verification of the recently upgraded spectrograph VLT/CRILES+ (Dorn et al. 2016). Our goal was a

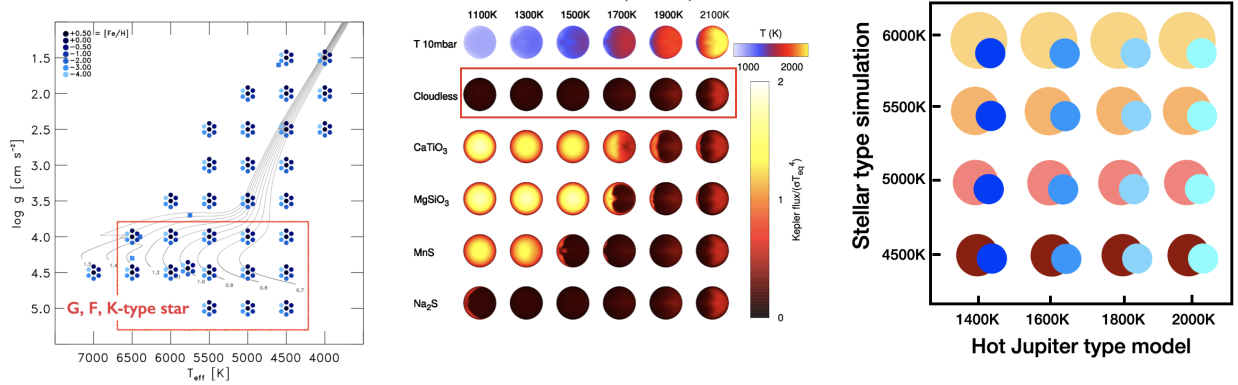


Fig. 2. *Left:* 3D RHD simulation-grid in the H-R diagram computed with STAGGER-CODE (Magic et al. 2013). In particular, the G,F and K stellar types (within the red line) are the ones used in this work. *Central:* Temperature and outgoing flux from the dayside of Hot Jupiters with different equilibrium temperatures and cloud species (Parmentier et al. 2016). Cloud-free models (within the red line) are the ones used in this work. *Right:* Estimated coupling grid of those stellar and planet models marked in the previous panels.

demonstration of the basic capabilities of the new instrument and we chose to observe WASP-20 because it was the only target with a visible transit during the SV observing window. The system was observed for the first time by Anderson et al. (2015), discovered as a binary system separated by only 0.26'' by Evans et al. (2016) and confirmed by Southworth et al. (2020).

Because with CRIFRES+ we did not resolve the binary nature of WASP-20 found by Evans et al. (2016) and Southworth et al. (2020), we treated the system as a single star and took as main reference Anderson et al. (2015). We used Principal Component Analysis (PCA, Murtagh & Heck 1987, Press et al. 1992) to remove any dominant time dependent contaminating features (such as telluric bands, stellar absorption lines and systematic instrumental trends) and we cross-correlated the residual spectra with models of the WASP-20b atmosphere to extract the planet spectrum, as done by Giacobbe et al. (2021). We used synthetic spectra computed from 1D models using GENESIS (Gandhi & Madhusudhan 2017), and from SPARC/MIT Global Circulation Models (GCM, Showman et al. 2013, Parmentier et al. 2021, Pluriel et al. 2022) using Pytmosph3R (Caldas et al. 2019, Falco et al. 2022). The best fitting model was a cloud-free GCM at 1400K containing only H₂O (VMR=-3.3), in

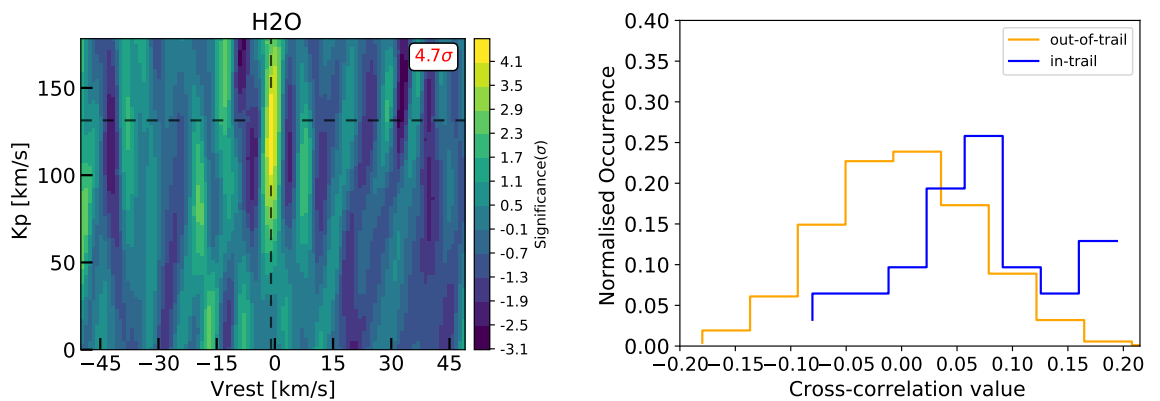


Fig. 3. *Left:* Total cross correlation signal from the GCM used for the atmosphere of WASP-20b in our analysis, shown as a function of rest-frame velocity and planet projected orbital velocity. The GCM is cloud-free, in chemical equilibrium with no thermal inversion and contains a VMR[H₂O] equals to -3.3. *Right:* Comparison between out-of-trail (yellow solid line) and in-trail (blue solid line) cross-correlation distributions of WASP-20b. The latter is systematically shifted towards higher. A Welch t-test on the data rejects the hypothesis that the two distributions are drawn from the same parent distribution at the 4.1σ.

chemical equilibrium and with no thermal inversion. The cross-correlation matrix (shown in Fig. 3, left panel) peaks at $K_P=131^{+23}_{-39}$ km s⁻¹ and $V_{\text{rest}}=-1 \pm 1$ km s⁻¹, in accordance with the RV semi-amplitude expected from Anderson et al. (2015) results.

We determined the statistical significance of the H₂O signal as in previous works (Brogi et al. 2012, Brogi et al. 2013). From the matrix containing the cross correlation signal as function of planet radial velocity and time, CCF(V, t), we selected those values not belonging to the planet RV curve (out-of-trail) and those ones belonging to the planetary trace (in-trail), as shown in Fig. 3, right panel. A Welch T-test ruled out the in-trail and out-of-trail values having been drawn from the same parent distribution at the 4.1σ level. More details will be found in Maimone et al. 2022 (submitted).

This project has received funding from the European Research Council (ERC) under the European Union's Horizon 2020 research and innovation programme (grant agreement no 679030/WHIPLASH).

References

- Anderson, D. R., Collier Cameron, A., Hellier, C., et al. 2015, *A&A*, 575, A61
- Birkby, J. L. 2018, arXiv e-prints, arXiv:1806.04617
- Brogi, M., Snellen, I. A. G., de Kok, R. J., et al. 2012, *Nature*, 486, 502
- Brogi, M., Snellen, I. A. G., de Kok, R. J., et al. 2013, *ApJ*, 767, 27
- Caldas, A., Leconte, J., Selsis, F., et al. 2019, *A&A*, 623, A161
- Cegla, H. M., Watson, C. A., Shelyag, S., Mathioudakis, M., & Moutari, S. 2019, *ApJ*, 879, 55
- Chiavassa, A. & Brogi, M. 2019, *A&A*, 631, A100
- Chiavassa, A., Caldas, A., Selsis, F., et al. 2017, *A&A*, 597, A94
- Chiavassa, A., Plez, B., Josselin, E., & Freytag, B. 2009, *A&A*, 506, 1351
- Dorn, R. J., Follert, R., Bristow, P., et al. 2016, in Society of Photo-Optical Instrumentation Engineers (SPIE) Conference Series, Vol. 9908, Ground-based and Airborne Instrumentation for Astronomy VI, ed. C. J. Evans, L. Simard, & H. Takami, 99080I
- Dravins, D., Ludwig, H.-G., & Freytag, B. 2021, *A&A*, 649, A17
- Evans, D. F., Southworth, J., & Smalley, B. 2016, *ApJ*, 833, L19
- Falco, A., Zingales, T., Pluriel, W., & Leconte, J. 2022, *A&A*, 658, A41
- Flowers, E., Brogi, M., Rauscher, E., Kempton, E. M. R., & Chiavassa, A. 2019, *AJ*, 157, 209
- Gandhi, S. & Madhusudhan, N. 2017, *MNRAS*, 472, 2334
- Giacobbe, P., Brogi, M., Gandhi, S., et al. 2021, *Nature*, 592, 205
- Madhusudhan, N. 2012, in EGU General Assembly Conference Abstracts, EGU General Assembly Conference Abstracts, 13720
- Magic, Z., Collet, R., Asplund, M., et al. 2013, *A&A*, 557, A26
- Murtagh, F. & Heck, A. 1987, *Multivariate Data Analysis*, Vol. 131
- Nordlund, Å., Stein, R. F., & Asplund, M. 2009, *Living Reviews in Solar Physics*, 6, 2
- Parmentier, V., Fortney, J. J., Showman, A. P., Morley, C., & Marley, M. S. 2016, *ApJ*, 828, 22
- Parmentier, V., Showman, A. P., & Fortney, J. J. 2021, *MNRAS*, 501, 78
- Pluriel, W., Leconte, J., Parmentier, V., et al. 2022, *A&A*, 658, A42
- Press, W. H., Teukolsky, S. A., Vetterling, W. T., & Flannery, B. P. 1992, *Numerical recipes in FORTRAN. The art of scientific computing*
- Showman, A. P., Fortney, J. J., Lewis, N. K., & Shabram, M. 2013, *ApJ*, 762, 24
- Snellen, I. A. G., de Kok, R. J., de Mooij, E. J. W., & Albrecht, S. 2010, *Nature*, 465, 1049
- Southworth, J., Bohn, A. J., Kenworthy, M. A., Ginski, C., & Mancini, L. 2020, *A&A*, 635, A74